Robotica (2003) volume 21, pp. 495–504. © 2003 Cambridge University Press
DOI: 10.1017/S0263574703005071 Printed in the United Kingdom

Polytopic gain scheduled H_∞ control for robotic manipulators

Zhongwei Yu,* Huitang Chen* and Peng-Yung Woo†

(Received in Final Form: February 6, 2003)

SUMMARY

A new approach to the design of a polytopic gain scheduled H_∞ controller with pole placement for n-joint rigid robotic manipulators is presented. With linearization around the equilibrium manifold, the robotic system is transformed into a continuous linear parameter-varying (LPV) system with respect to the equilibrium manifold. A filter is introduced to obtain an augmented system, which is apt to have the polytopic gain scheduled controller designed. This system is put into a polytopic expression by a convex decomposition. Based on the concepts of quadratic D-stability and quadratic H_∞ performance, the polytopic features are used to simplify the controller design to be a vertices' controller design for the polytope. A state feedback gain, which satisfies H_∞ performance and dynamic characteristics for each vertex of the polytope, is designed with a Linear Matrix Inequality (LMI) approach. A global continuous gain scheduled controller is then obtained by a synthesis of the vertex gains. Experiments demonstrate the feasibility of the designed controller.

KEYWORDS: Polytopic gain scheduled control; Manipulators; LMI approach; Vertex gains.

1. INTRODUCTION

As a highly-coupled nonlinear system, the dynamics of a manipulator changes along with the change of the manipulator's geometric features and inertia. Moreover, there are model errors in modeling the robotic manipulator (e.g. the unmodeled part in the high frequency range) and dynamic uncertainties and external disturbances (e.g., the coupling among joints, frictions, noise in sensors and executors etc). In order to guarantee good dynamic characteristics in the whole motion region, the controller design needs to attain two objects, i.e. the disturbance attenuation and robust stability, and the real-time adjustment of the controller dynamics along with the change of the manipulator's geometric features and inertia. The first object can be attained by H_∞ synthesis techniques.[1] It is necessary to use gain schedule technique for the second object.[2] However, the existing robotic control schemes, such as the adaptive control,[3,4] the H_∞ control,[5,6] the fuzzy control[7] and the neural network control,[8] work for only one of the objects. To have a combination of the two aforementioned objects is one of the topics in our research presented in this article.

* Information and Control Engineering Dept., Tongji University, Shanghai (China)
† Electrical Engineering Dept., Northern Illinois University, Dekalb IL 60115 (USA)

In a conventional gain scheduled control,[9–11] a nonlinear system is linearized to be segments of linear subsystems at different motion regions. In each of the linear region, a state feedback gain is designed by using a certain linear robust control method. The controller keeps on testing the system states, deciding the motion regions and using the corresponding gain control systems. For the conventional gain scheduled controllers, it is required that the system states do not change too fast, since a fast varying system means a fast pass through the motion regions, which results in the fast switching of the gains. In order to capture the nonlinearity of the original system, the switching standard for the different gains must be appropriately chosen. If the switching standard is too coarse, the system performance becomes poor and system stability is affected, especially during the transition from one motion region to another. On the other hand, if the regions are divided too finely, though the system performance is improved and the system stability is increased, a large amount of space is needed to store the gains for the different motion regions. Therefore, it is concluded that the conventional gain scheduled controllers are only good for slow varying systems. Moreover, the design of the conventional gain scheduled controllers does not take into consideration of the time-varying property of the system and does not have a theoretical basis for the system stability and performance in the whole range of the varying-parameters. Also, it usually takes a big off-line computation load. These are fatal deficiencies of the conventional gain scheduled controllers.

In order to overcome the aforementioned deficiency, the polytope technique is proposed in this article. The linearized state equation of the manipulator is expressed by a polytope. Since it is a convex set, the polytope can be described completely by the vertices. Thus, in the controller design, it is unnecessary to have designs with respect to all the points in the polytope. Computation load is much reduced, since only designs with respect to the vertices are needed. At the same time, continuous gains of the controller are obtained.

From the viewpoint of digital realization, fast controller dynamics must be prevented. The used approach of the feature weighting function is not feasible in practical applications due to the resulted high-order controllers. In this article, the multi-object expansion of polytope technique is proposed. Pole placement requirement is added in the H_∞ design so that the closed-loop poles are arranged to enter into the appropriate regions in the left-half plane to achieve satisfactory time response and closed-loop damping. Thus, large closed-loop poles are eliminated to prevent fast controller dynamics.

Recently, the Linear Matrix Inequality (LMI), due to its highly efficient solutions, has attracted the attention of the

control area and become an important method in robust control analysis and design. The LMI method makes the H_∞ synthesis become a problem of convex optimization.[12] Essentially, the LMIs present a constrain relationship, which offers more flexibility for combining some constraints in the closed-loop system, and is suitable to multi-object controllers such as H_∞ and pole placement. The LMIs can be solved efficiently by interior-point optimization algorithms,[13] especially the MATLAB *LMI Control Toolbox*.[14]

A new approach to the design of a polytopic gain scheduled H_∞ controller with pole placement for n-joint rigid robotic manipulators is presented. With linearization around the equilibrium manifold, the robotic system is transformed into a continuous linear parameter-varying (LPV) system with respect to the equilibrium manifold. A filter is introduced to obtain an augmented system, which is apt to have the polytopic gain scheduled controller designed. This system is put into a polytopic expression by a convex decomposition. Based on the concepts of quadratic D-stability and quadratic H_∞ performance, the polytopic features are used to simplify the controller design to be a vertices' controller design for the system polytope. By combining H_∞ and pole placement object, a state feedback gain which satisfies H_∞ performance and dynamic characteristics for each vertex of the system polytope is designed with a LMI approach.[15] A global continuous gain scheduled controller is then obtained by a synthesis of the vertex gains.

2. THE LPV TRANSFORMATION OF A ROBOTIC SYSTEM AND ITS POLYTOPIC EXPRESSION

The dynamics equation of an n-joint rigid robotic manipulator is

$$M(q)\ddot{q}+C(q,\dot{q})\dot{q}+g(q)=\tau \tag{1}$$

where $q\in R^n$ is the joint position vector, $M(q)\in R^{n\times n}$ is the inertia matrix, $C(q,\dot{q})\dot{q}\in R^n$ is the centrifugal and Couliaulis term, $g(q)\in R^n$ is the gravity term and $\tau\in R^n$ is the control torque.

Suppose $x_1=q$, $x_2=\dot{q}$ and $\overline{X}=(x_1\ \ x_2)^T$. (1) can be expressed in a state space as

$$\dot{\overline{X}}=F(\overline{X})+G(\overline{X})\tau \tag{2}$$

where $$F(\overline{X})=\begin{bmatrix}[0_{n\times n}\ \ I_{n\times n}]\overline{X}\\ -M^{-1}(\overline{X})(C(\overline{X})+g(\overline{X}))\end{bmatrix}$$

and $$G(\dot{\overline{X}})=\begin{bmatrix}0_{n\times 1}\\ M^{-1}(\overline{X})\end{bmatrix}.$$

For system (2), a varying-parameter $\rho(t)=[\rho_1(t),\ldots,\rho_l(t)]^T\subset R^l[\rho(t)$ is written as ρ for simplicity in the following text] is selected with its vertex set being $\mathbf{V}:=\{\omega_1,\ldots,\omega_N\}$ where $\omega_i\in R^l$, $i=1,\ldots,N$. After convex decomposition, the varying-parameter ρ changes in the polytope with its vertex set being V, i.e., $\rho=\sum_{i=1}^{N}\mu_i(\rho)\omega_i$ where, $\mu_i(\rho)\geq 0$, $\sum_{i=1}^{N}\mu_i(\rho)=1$.

Assume that there is an equilibrium manifold parameterized by the varying-parameter ρ, i.e., there is a continuous function $\overline{X}_e(\rho)$: $R^l\rightarrow R^n$ and $\tau_e(\rho)$: $R^l\rightarrow R^n$ such that for all ρ, which has a vertex set V we have

$$0=F(\overline{X}_e(\rho))+G(\overline{X}_e(\rho))\tau_e(\rho) \tag{3}$$

where the varying-parameter ρ could be the function of the system states, the inputs, the outputs or the external signals. For a specified plant, the selection of the varying-parameter ρ is not unique. The selection principle is that the selected ρ is able to reflect the dynamic characteristics of the original system. For every ρ at the equilibrium manifold (3), (2) can be reduced, after a Jacobian linearization, to

$$\dot{\hat{x}}(t)=\hat{A}(\rho)\hat{x}(t)+\hat{B}(\rho)\hat{u}(t) \tag{4}$$

where $\hat{x}(t)=\overline{X}(t)-\overline{X}_e(\rho)$ $\hat{u}(t)=\tau(t)-\tau_e(\rho)$,

$\hat{A}(\rho)=\dfrac{\partial}{\partial X}(F(\overline{X})+G(\overline{X})\tau)\,|_{\overline{X}_e(\rho),\tau_e(\rho)}$ and $\hat{B}(\rho)=G(\overline{X}_e(\rho))$ in which $\hat{A}(\rho)$ and $\hat{B}(\rho)$ are the affine functions of the varying-parameter ρ, i.e., $[\hat{A}(\rho)\hat{B}(\rho)]=\sum_{i=1}^{l}\rho_i[\hat{A}_i\ \hat{B}_i]$, which can be obtained by an appropriate selection of the varying-parameter ρ.

Equation (4) is the LPV expression of the robotic system. Since there are model errors such as the high-frequency unmodeled part in robotic modeling and the dynamic uncertainty and external disturbance in robotic motion such as joint coupling, friction, and sensor and executor noise, an equivalent disturbance $w_i(t)$ for the model errors, the dynamic uncertainty and external disturbance is added in (4) and then (4) is written as

$$\dot{\hat{x}}(t)=\hat{A}(\rho)\hat{x}(t)+\hat{B}_1 w(t)+\hat{B}_2(\rho)\hat{u}(t) \tag{5}$$

where $\hat{B}_1=\begin{bmatrix}0_{n\times n}\\ I_{n\times n}\end{bmatrix}$, $\hat{B}_2(\rho)=\hat{B}(\rho)$.

In (5), $\hat{B}_2(\rho)$ is the affine function of the varying-parameter ρ and therefore it is difficult to design the gain-scheduled controller by using the polytopic technique, since this system does not have the vertex property mentioned in Theorem 1. A 1st-order filter is introduced to solve this problem in this paper. Hereby define a new control input u and the state equation of the filter is:

$$\begin{aligned}\dot{x}_u&=A_u X_u+B_u u\\ \hat{u}&=C_u x_u\end{aligned} \tag{6}$$

where the coefficient matrices $A_u\in R^{n\times n}$, $B_u\in R^{n\times n}$ and $C_u\in R^{n\times n}$ are the filter design parameters. In the filter design, the bandwidth is required to be broader than the expected

https://doi.org/10.1017/S0263574703005071 Published online by Cambridge University Press

system bandwidth. Define $x=[\hat{x}\ x_u]^T$. Combining (5) and (6), the augmented plant can be expressed as

$$\dot{x}=A(\rho)x+B_1w+B_2u \tag{7}$$

where $A(\rho)=\begin{bmatrix}\hat{A}(\rho) & \hat{B}_2(\rho)C_u\\ 0 & A_u\end{bmatrix}=\begin{bmatrix}\sum_{i=1}^{l}\rho_i\hat{A}_i & \sum_{i=1}^{l}\rho_i\hat{B}_iC_u\\ 0 & A_u\end{bmatrix}$,

$$B_1=\begin{bmatrix}0_{n\times n}\\ I_{n\times n}\\ 0_{n\times n}\end{bmatrix} \text{ and } B_2=\begin{bmatrix}0_{n\times n}\\ B_{n\times n}\end{bmatrix}.$$

It is seen that after the filter is introduced, matrix B_2 in the augmented plant (7) becomes a constant matrix. For such a kind of structure, a gain-scheduled controller by using the polytopic technique can be designed. While the performance index $Z(t)\in R^{k\times 1}$ expresses the disturbance-attenuation performance for disturbance w(t), (7) can further be expanded to be a LPV system:

$$P(\rho):\begin{matrix}\dot{x}(t)=A(\rho)x(t)+B_1w(t)+B_2u(t)\\ Z(t)=C_1x(t)+D_1u(t)\end{matrix} \tag{8}$$

where the coefficient matrices C_1 and D_1 of the performance index satisfy $C_1^TC_1=P$ and $D_1^TD_1=Q$, where $P>0$ and $Q>0$ are the weighting matrices. C_1 and D_1 are obtained based on the requirement that the closed-loop system possesses the H_∞ performance γ for any disturbance

$$w\in L_2[0,+\infty), \text{ i.e., } \frac{1}{\gamma}\int_0^\infty (x^TPx+u^TQu)dt<\gamma\int_0^\infty w^Twdt$$

Since the varying-parameter ρ changes in the fixed polytope with its vertex set being $\mathbf{V}$ and $A(\rho)$ in system (8) is also the affme function of the varying-parameter ρ, the state-space matrices in system (8) change in a matrix polytope, i.e.

$$\begin{bmatrix}A(\rho) & B_1 & B_2\\ C_1 & 0 & D_1\end{bmatrix}=\sum_{i=1}^{N}\mu_i(\rho)\begin{bmatrix}A(\omega_i) & B_1 & B_2\\ C_1 & 0 & D_1\end{bmatrix}:$$

$$=\sum_{i=1}^{N}\mu_i(\rho)\begin{bmatrix}A_i & B_1 & B_2\\ C_1 & 0 & D_1\end{bmatrix}$$

$$\mu_i(\rho)\geq 0,\ \sum_{i=1}^{N}\mu_i(\rho)=1$$

Thus, (8) is the polytopic expression of the robotic system with a LPV transformation.

3. THE DESIGN OF THE POLYTOPIC GAIN SCHEDULED H_∞ CONTROLLER

3.1. Related definitions and theorems

Definition 1 (the LMI region).[15]
Suppose D is a subset of a complex plane. If there exists a symmetric matrix $\alpha=[\alpha_{kl}]\in R^{m\times m}$ and a matrix $\beta=[\beta_{kl}]\in R^{m\times m}$ such that $D=\{z\in C: f_D(z)<0\}$, where $f_D(z):=\alpha+z\beta+\bar{z}\beta^T=[\alpha_{kl}+\beta_{kl}z+\beta_{lk}\bar{z}]_{1\leq k,l\leq m}$ is the characteristic function of D and takes value in the $m\times m$ Hermitian matrix space, then D is called a LMI region.

In the above definition, $M=[\mu_{kl}]_{1\leq k,l\leq m}$ expresses that M is an $m\times m$ matrix with a general term μ_{kl}.

Definition 2 (Quadratic D-stability).
Suppose that for the LPV system $\dot{x}=A(p)x$ with respect to p, when p is a fixed value, its pole location in the LMI region D can be described in the following:

$$M_D(A(p),X)=[\alpha_{kl}X+\beta_{kl}A(p)X+\beta_{lk}XA(p)^T]_{1\leq k,l\leq m}$$

where X is a positive definite matrix, $M_D(A(p), X)$ and $f_D(z)$ can be related by the following substitution (X, $A(p)X$, $XA(p)^T$) $\leftrightarrow$ (1, z, $\bar{z}$). Then, the matrix $A(p)$ is quadratic D-stable if and only if there exists a symmetric positive definite matrix X such that $M_D(A(p), X)<0$ for all admissible values of the parameter p.

Definition 3 (Quadratic H_∞ performance).
For the LPV system with respect to p

$$\begin{matrix}\dot{x}=A(p)x+B(p)u\\ y=C(p)X+D(p)u\end{matrix} \tag{9}$$

has quadratic H_∞ performance γ if and only if there exists a positive definite matrix $X>0$ such that

$$B^O_{[A(p),B(p),C(p),D(p)]}(X,\gamma):=\begin{bmatrix}A^T(p)X+XA(p) & XB(p) & C^T(p)\\ B^T(p)X & -\gamma I & D^T(p)\\ C(p) & D(p) & -\gamma I\end{bmatrix}<0$$

for all admissible values of the parameter p.

Theorem 1 (Vertex property).
For the polytopic linear parameter-varying plant (9), where the varying-parameter ρ changes in the polytope with $\omega_1, \cdots, \omega_r$ as its vertices, i.e.,

$$p\in C_O(\omega_1,\cdots,\omega_r)=\left\{\sum_{i=1}^{r}\alpha_i\omega_i:\alpha_i\geq 0,\ \sum_{i=1}^{r}\alpha_i=1\right\}$$

and the state space matrix changes in a matrix polytope, i.e.,

$$\begin{bmatrix}A(p) & B(p)\\ C(p) & D(p)\end{bmatrix}\in P:=C_O\left\{\begin{bmatrix}A_i & B_i\\ C_i & D_i\end{bmatrix},\ i=1,\cdots,r\right\},$$

the following three items are equivalent:

https://doi.org/10.1017/S0263574703005071 Published online by Cambridge University Press

(1) The system is quadratic D-stable with quadratic H_∞ performance γ.
(2) There exists a positive definite matrix $X>0$ such that for

$$\text{all} \begin{bmatrix} A(p) & B(p) \\ C(p) & D(p) \end{bmatrix} \in P,$$

$$M_{\mathrm{D}}(A(p), X)<0$$

$$B^{o}_{[A(p),B(p),C(p),D(p)]}(X,\gamma)<0$$

(3) There exists a positive definite matrix $X>0$, which satisfies the following LMIs:

$$\begin{matrix} M_{\mathrm{D}}(A_i, X)<0 \\ B^{o}_{[A_i,B_i,C_i,D_i]}(X,\gamma)<0 \end{matrix} \quad i=1, 2, \cdots, r$$

Proof:
According to Definitions 2 and 3, it is evident (1) and (2) are equivalent. Let us now prove the equivalence of (2) and (3). When (2) holds, the polytopic vertices satisfy (3), i.e., (3) holds. On the other hand, we noticed that

$$\begin{bmatrix} A(p) & B(p) \\ C(p) & D(p) \end{bmatrix} = \sum_{i=1}^{r} \alpha_i \begin{bmatrix} A_i & B_i \\ C_i & D_i \end{bmatrix}, \quad \text{where} \quad \alpha_i \geq 0 \quad \text{and}$$

$\sum_{i=1}^{r} \alpha_i = 1$. Then $M_{\mathrm{D}}(A(p), X) = \sum_{i=1}^{r} \alpha_i M_{\mathrm{D}}(A_i, X)$ and

$B^{o}_{[A(p),B(p),C(p),D(p)]}(X,\gamma) = \sum_{i=1}^{r} \alpha_i B^{o}_{[A_i,B_i,C_i,D_i]}(X,\gamma)$. Therefore if (3) holds, (2) holds too.

3.2. The design of the polytopic controller
For the polytopic LPV system (8), we design a gain scheduled state feedback controller with a same polytopic structure:

$$u = K(\rho)x \tag{10}$$

where $K(\rho) = \sum_{i=1}^{N} \mu_i(\rho) K_i$ and K_i is the vertex of the polytopic controller.

The following theorem proves the feasibility of this design.

Theorem 2.
In the design of the state feedback controller (10) for a system expressed by (8), if there exists a positive definite matrix $X>0$ such that K_i satisfies $M_{\mathrm{D}}(A_i+K_i, X)<0$ and $B^{o}_{[A_i+K_i,B_1,C_1+D_{12}K_i,0]}(X,\gamma)<0$, $i=1, \ldots, N$, the designed polytopic controller (10) guarantees that the closed-loop system is quadratic D-stable and has a quadratic H_∞ performance γ between $w(t)$ and $Z(t)$ for all admissible values of the varying-parameter ρ.

Proof:
Let the controller (10) be put into the system (8). The closed-loop system is

$$\begin{aligned} \dot{x}_{cl} &= \left\{ \sum_{i=1}^{N} \mu_i(\rho)(A_i + B_2 K_i) \right\} x_{cl} + B_1 w \\ Z &= \left\{ \sum_{i=1}^{N} \mu_i(\rho)(C_1 + D_{12} K_i) \right\} x_{cl} \end{aligned} \tag{11}$$

It is seen that the closed-loop system has also a polytopic structure. According to Theorem 1, for LPV system (8) with a polytopic structure, as long as all the polytopic vertices satisfy $M_{\mathrm{D}}(A_i+K_i, X)<0$ and $B^{o}_{[A_i+K_i,B_1,C_1+D_{12}K_i,0]}(X,\gamma)<0$, $i=1, \ldots, N$, the polytopic controller (10) guarantees the closed-loop system is quadratic D-stable and has a quadratic H_∞ performance γ between $w(t)$ and $Z(t)$ for all admissible values of the varying parameter ρ.

Theorem 2 reveals that the key to the design of the polytopic controller is to find a positive definite matrix $X>0$ and the vertices' controllers K_i. We use LMI technique to solve the problem. Figure 1 demonstrates the design principle for the polytopic controller.

3.3. The design of the vertices' controllers
From the polytopic parameter-varying system (8), the linear time-invariant (LTI) systems at the vertices are

$$\begin{matrix} \dot{x} = A_i x + B_1 w + B_2 u \\ Z = C_1 x + D_{12} u \end{matrix} \quad i=1, \ldots, N \tag{12}$$

Suppose $T_{wzi}(s)$ is the closed-loop transfer function between $w(t)$ and $z(t)$, and its closed-loop realization is $(A_{cli}, B_{cli}, C_{cli}, D_{cli})$. To obtain satisfied dynamic characteristics, the closed-loop poles are required to be placed in the region $S(\alpha, r, \theta)$ in Figure 2. Confining the closed-loop poles in this region ensures a minimum decay rate α, a minimum

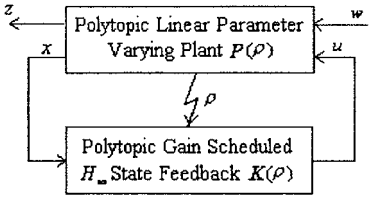

Fig. 1. The design principle of the polytopic controller.

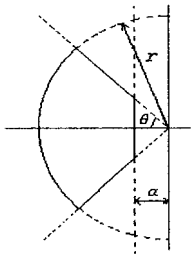

Fig. 2. The pole-placement region $S(\boldsymbol{a, r,} \theta)$.

https://doi.org/10.1017/S0263574703005071 Published online by Cambridge University Press

damping ratio $\xi=\cos\theta$, and a maximum undamped natural frequency $\omega_d=r\sin\theta$ within a certain scope. These, in turn, bound the maximum overshoot, the frequency of oscillation, the decay time, the rise time and the settling time. As is seen from Definition 1, region $S(\alpha, r, \theta)$ is a LMI region.

Theorem 3.
Given $\gamma>0$, there exists a positive-definite symmetric matrix X and $L_i=K_iX$, which satisfy the following LMIs:

$$A_iX+XA_i^T+B_2L_i+L_i^TB_2^T<(-2\alpha)X \tag{13}$$

$$\begin{bmatrix} -rX & A_iX+B_2L_i \\ XA_i^T+L_i^TB_2^T & -rX \end{bmatrix}<0 \tag{14}$$

$$\begin{bmatrix} I_{11i} & I_{12i} \\ I_{21i} & I_{22i} \end{bmatrix}<0 \tag{15}$$

$$\begin{bmatrix} A_iX+XA_i^T+B_2L_i+L_i^TB_2^T & B_1 & XC_1^T+L_i^TD_{12}^T \\ B_1^T & -\gamma & D_{11}^T \\ C_1X+D_{12}L_i & D_{11} & -\gamma \end{bmatrix}<0 \tag{16}$$

where

$$I_{11i}=\sin\theta\cdot A_iX+X(\sin\theta\cdot A_i)^T+(\sin\theta\cdot B_2)L_i+L_i^T(\sin\theta\cdot B_2)^T$$

$$I_{21i}=\cos\theta\cdot A_iX-\cos\theta\cdot XA_i^T+\cos\theta\cdot B_2L_i-\cos\theta\cdot L_i^TB_2^T$$

$$I_{12i}=I_{21i}^T$$

$$I_{22i}=I_{11i}$$

$$i=1,\ldots,N$$

Suppose (X^*, L^*) is one feasible solution of the above LMIs. Then the matrix X^* and the feedback gain $K_i^*=L_i^*(X^*)^{-1}$ are the positive definite matrix $X_{cl}>0$ and the vertices' controllers, respectively, which satisfy Theorem 2.

Proof:
For the pole-placement region $S(\alpha, r, \theta)$ as shown in Figure 2, according to the relationship between $M_D(A, X)$ and $f_D(z)$, the following LMIs, which satisfy the pole-placement requirements, can be obtained from Definition 2 and Theorem 1: there exists $X_D>0$ such that

$$A_{cli}X_D+X_DA_{cli}^T+2\alpha X_D<0 \tag{17}$$

$$\begin{bmatrix} -rX_D & A_{cli}X_D \\ X_DA_{cli}^T & -rX_D \end{bmatrix}<0 \tag{18}$$

$$\begin{bmatrix} \sin\theta(A_{cli}X_D+X_DA_{cli}^T) & \cos\theta(A_{cli}X_D-X_DA_{cli}^T) \\ \cos\theta(X_DA_{cli}^T-A_{cli}X_D) & \sin\theta(A_{cli}X_D+X_DA_{cli}^T) \end{bmatrix}<0 \tag{19}$$

Also, from Definition 3 and Theorem 1, the LMI, which guarantees $T_{wzi}(s)$ to possess a quadratic H_∞ performance $\|T_{wzi}\|_\infty<\gamma$, is: there exists $X_\infty>0$ such that

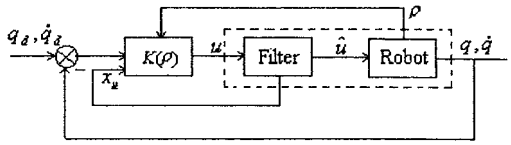

Fig. 3. The block diagram of the closed-loop control.

$$\begin{bmatrix} A_{cli}X_\infty+X_\infty A_{cli}^T & B_{cli} & X_\infty C_{cli}^T \\ B_{cli}^T & -\gamma I & D_{cli}^T \\ C_{cli}X_\infty & D_{cli} & -\gamma I \end{bmatrix}<0 \tag{20}$$

From (11), $A_{cli}=A_i+B_2K_i$, $B_{cli}=B_1$, $C_{cli}=C_1+D_{12}K_i$ and $D_{cli}=0$. Suppose $X=X_D=X_\infty>0$, and $L_i=K_iX$. With the substitution of the above into (17)–(20), it is easy to obtain (13)–(16).

The above inequality constraints can be easily solved by some LMI optimization software, such as MATLAB *LMI Control Toolbox*.[14] It is worth noticing that all the feedback gains for the vertices are obtained off-line. Real-time calculation is only for (12). Therefore, in practical control, the proposed controller in this paper has a small on-line computation load and thus is easy to be realized. See Figure 3 for the overall control scheme.

4. EXPERIMENTS

Experimental studies are carried out on a self-designed direct drive two-joint planar robotic manipulator (DDR) shown in Figure 4.

The dynamics equation of the manipulator is expressed as[16]

$$\begin{bmatrix} a & b\cos(\theta_2-\theta_1) \\ b\cos(\theta_2-\theta_1) & c \end{bmatrix}\cdot\begin{bmatrix} \ddot{\theta}_1 \\ \ddot{\theta}_2 \end{bmatrix} + \begin{bmatrix} -b\dot{\theta}_2^2\sin(\theta_2-\theta_1) \\ b\dot{\theta}_1^2\sin(\theta_2-\theta_1) \end{bmatrix}=\begin{bmatrix} \tau_1 \\ \tau_2 \end{bmatrix} \tag{21}$$

where $a=5.6794\ kg\cdot m^2$, $b=1.4730\ kg\cdot m^2$ and $c=1.7985\ kg\cdot m^2$.

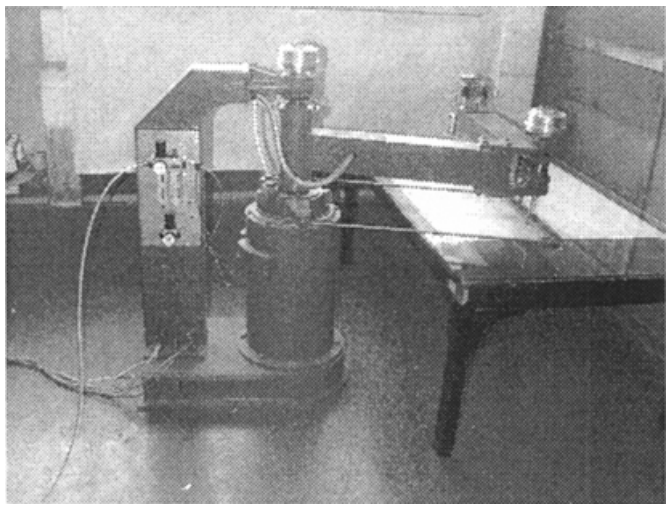

Fig. 4. The direct-drive robotic manipulator.

https://doi.org/10.1017/S0263574703005071 Published online by Cambridge University Press

Defining $M=ac-b^2\cos^2(\theta_2-\theta_1)$, from (21) we obtain

$$\ddot{\theta}_1=\frac{bc\dot{\theta}_2^2\sin(\theta_2-\theta_1)+\frac{1}{2}b^2\dot{\theta}_1^2\sin 2(\theta_2-\theta_1)}{M}+\frac{c\tau_1-b\cos(\theta_2-\theta_1)\tau_2}{M} \tag{22}$$

$$\ddot{\theta}_2=\frac{-ab\dot{\theta}_1^2\sin(\theta_2-\theta_1)-\frac{1}{2}b^2\dot{\theta}_2^2\sin 2(\theta_2-\theta_1)}{M}+\frac{a\tau_2-b\cos(\theta_2-\theta_1)\tau_1}{M} \tag{23}$$

Then

$$\frac{\partial\ddot{\theta}_1}{\partial\theta_1}=\frac{-bc\dot{\theta}_2^2\cos(\theta_2-\theta_1)-b^2\dot{\theta}_1^2\cos 2(\theta_2-\theta_1)-b\sin(\theta_2-\theta_1)\tau_2}{M}+\frac{b^2\sin 2(\theta_2-\theta_1)\left[bc\dot{\theta}_2^2\sin(\theta_2-\theta_1)+\frac{1}{2}b^2\dot{\theta}_1^2\sin 2(\theta_2-\theta_1)\right.}{M^2}\left.\frac{+c\tau_1-b\cos(\theta_2-\theta_1)\tau_2\right]}{M^2}$$

$$\frac{\partial\ddot{\theta}_1}{\partial\theta_2}=\frac{bc\dot{\theta}_2^2\cos(\theta_2-\theta_1)+b^2\dot{\theta}_1^2\cos 2(\theta_2-\theta_1)+b\sin(\theta_2-\theta_1)\tau_2}{M}+\frac{b^2\sin 2(\theta_2-\theta_1)\left[bc\dot{\theta}_2^2\sin(\theta_2-\theta_1)+\frac{1}{2}b^2\dot{\theta}_1^2\sin 2(\theta_2-\theta_1)\right.}{M^2}\left.\frac{+c\tau_1-b\cos(\theta_2-\theta_1)\tau_2\right]}{M^2}$$

$$\frac{\partial\ddot{\theta}_1}{\partial\dot{\theta}_1}=\frac{b^2\dot{\theta}_1\sin 2(\theta_2-\theta_1)}{M}$$

$$\frac{\partial\ddot{\theta}_1}{\partial\dot{\theta}_2}=\frac{2bc\dot{\theta}_2\sin(\theta_2-\theta_1)}{M}$$

$$\frac{\partial\ddot{\theta}_1}{\partial\tau_1}=\frac{c}{M}$$

$$\frac{\partial\ddot{\theta}_1}{\partial\tau_2}=\frac{-b\cos(\theta_2-\theta_1)}{M}$$

$$\frac{\partial\ddot{\theta}_2}{\partial\theta_1}=\frac{ab\dot{\theta}_1^2\cos(\theta_2-\theta_1)+b^2\dot{\theta}_2^2\cos 2(\theta_2-\theta_1)-b\sin(\theta_2-\theta_1)\tau_1}{M}+\frac{b^2\sin 2(\theta_2-\theta_1)\left[-ab\dot{\theta}_1^2\sin(\theta_2-\theta_1)-\frac{1}{2}b^2\dot{\theta}_2^2\sin 2(\theta_2-\theta_1)\right.}{M^2}\left.\frac{+a\tau_2-b\cos(\theta_2-\theta_1)\tau_1\right]}{M^2}$$

$$\frac{\partial\ddot{\theta}_2}{\partial\theta_2}=\frac{-ab\dot{\theta}_1^2\cos(\theta_2-\theta_1)-b^2\dot{\theta}_2^2\cos 2(\theta_2-\theta_1)+b\sin(\theta_2-\theta_1)\tau_1}{M}+\frac{-b^2\sin 2(\theta_2-\theta_1)\left[-ab\dot{\theta}_1^2\sin(\theta_2-\theta_1)-\frac{1}{2}b^2\dot{\theta}_1^2\sin 2(\theta_2-\theta_1)\right.}{M^2}\left.\frac{+a\tau_2-b\cos(\theta_2-\theta_1)\tau_1\right]}{M^2}$$

$$\frac{\partial\ddot{\theta}_2}{\partial\dot{\theta}_1}=\frac{-2ab\dot{\theta}_1\sin(\theta_2-\theta_1)}{M}$$

$$\frac{\partial\ddot{\theta}_2}{\partial\dot{\theta}_2}=\frac{-b^2\dot{\theta}_2\sin 2(\theta_2-\theta_1)}{M}$$

$$\frac{\partial\ddot{\theta}_2}{\partial\tau_1}=\frac{-b\cos(\theta_2-\theta_1)}{M}$$

$$\frac{\partial\ddot{\theta}_2}{\partial\tau_2}=\frac{a}{M}$$

At the equilibrium manifold $X_e=(\theta_{1e}\ \theta_{2e}\ \dot{\theta}_{1e}\ \dot{\theta}_{2e})^T=(\theta_{1e}\ \theta_{2e}\ 0+0)^T$ and $\tau_e=(0\ 0)^T$, let us linearize (22) and (23). Since

$$\frac{\partial\ddot{\theta}_1}{\partial\theta_1}\Big|_{(X_e,\tau_e)}=0,\ \frac{\partial\ddot{\theta}_1}{\partial\theta_2}\Big|_{(X_e,\tau_e)}=0,\ \frac{\partial\ddot{\theta}_1}{\partial\dot{\theta}_1}\Big|_{(X_e,\tau_e)}=0,\ \frac{\partial\ddot{\theta}_1}{\partial\dot{\theta}_2}\Big|_{(X_e,\tau_e)}=0,$$

$$\frac{\partial\ddot{\theta}_2}{\partial\theta_1}\Big|_{(X_e,\tau_e)}=0,\ \frac{\partial\ddot{\theta}_2}{\partial\theta_2}\Big|_{(X_e,\tau_e)}=0,\ \frac{\partial\ddot{\theta}_2}{\partial\dot{\theta}_1}\Big|_{(X_e,\tau_e)}=0,\ \frac{\partial\ddot{\theta}_2}{\partial\dot{\theta}_2}\Big|_{(X_e,\tau_e)}=0,$$

$$\frac{\partial\ddot{\theta}_1}{\partial\tau_1}\Big|_{(X_e,\tau_e)}=\frac{c}{ac-b^2\cos^2(\theta_{2e}-\theta_{1e})},$$

$$\frac{\partial\ddot{\theta}_1}{\partial\tau_2}\Big|_{(X_e,\tau_e)}=\frac{-b\cos(\theta_{2e}-\theta_{1e})}{ac-b^2\cos^2(\theta_{2e}-\theta_{1e})},$$

$$\frac{\partial\ddot{\theta}_2}{\partial\tau_1}\Big|_{(X_e,\tau_e)}=\frac{-b\cos(\theta_{2e}-\theta_{1e}}{ac-b^2\cos^2(\theta_{2e}-\theta_{1e})},$$

$$\frac{\partial\ddot{\theta}_2}{\partial\tau_2}\Big|_{(X_e,\tau_e)}=\frac{a}{ac-b^2\cos^2(\theta_{2e}-\theta_{1e})},$$

the linearized equation is

https://doi.org/10.1017/S0263574703005071 Published online by Cambridge University Press

$$\begin{bmatrix}\dot{\hat{\theta}}_1\\ \dot{\hat{\theta}}_2\\ \ddot{\hat{\theta}}_1\\ \ddot{\hat{\theta}}_2\end{bmatrix}=\begin{bmatrix}0&0&1&0\\0&0&0&1\\0&0&0&0\\0&0&0&0\end{bmatrix}\begin{bmatrix}\hat{\theta}_1\\ \hat{\theta}_2\\ \dot{\hat{\theta}}_1\\ \dot{\hat{\theta}}_2\end{bmatrix}+\begin{bmatrix}0&0\\0&0\\\dfrac{c}{M_e}&\dfrac{-b\cos(\theta_{2e}-\theta_{1e})}{M_e}\\\dfrac{-b\cos(\theta_{2e}-\theta_{1e})}{M_e}&\dfrac{a}{M_e}\end{bmatrix}\begin{bmatrix}\hat{\tau}_1\\ \hat{\tau}_2\end{bmatrix} \quad (24)$$

where $\hat{\theta}_1=\theta_1-\theta_{1e}$, $\hat{\theta}_2=\theta_2-\theta_{2e}$, $\dot{\hat{\theta}}_1=\dot{\theta}_1-\dot{\theta}_{1e}=\dot{\theta}_1$, $\dot{\hat{\theta}}_2=\dot{\theta}_2-\dot{\theta}_{2e}=\dot{\theta}_2$, $\hat{\tau}_1=\tau_1-\tau_{1e}=\tau_1$, $\hat{\tau}_2=\tau_2-\tau_{2e}=\tau_2$, and $M_e=ac-b^2\cos^2(\theta_{2e}-\theta_{1e})$.

Since $ac>>b^2$, $M_e\approx ac$. (24) can be written as:

$$\dot{\hat{x}}=A\hat{x}+B\hat{u} \quad (25)$$

where $A=\begin{bmatrix}0&0&1&0\\0&0&0&1\\0&0&0&0\\0&0&0&0\end{bmatrix}$,

$$B=\begin{bmatrix}0&0\\0&0\\\dfrac{1}{a}&-\dfrac{b}{ac}\cos(\theta_{2e}-\theta_{1e})\\-\dfrac{b}{ac}\cos(\theta_{2e}-\theta_{1e})&\dfrac{1}{c}\end{bmatrix},$$

$\hat{x}=(\hat{\theta}_1\ \ \hat{\theta}_2\ \ \dot{\hat{\theta}}_1\ \ \dot{\hat{\theta}}_2)^T$ and $\hat{u}=(\hat{\tau}_1\ \ \hat{\tau}_2)^T$.

It is seen from (25) that matrix B is the linear function of $\cos(\theta_{2e}-\theta_{1e})$, where $\theta_{2e}-\theta_{1e}$ is the angle between joint 1 and joint 2 in Figure 5. This angle decides the dynamic characteristics of (25). Practically, the measured values of θ_2 and θ_1 can be regarded as the equilibrium points to linearize the system (21). Thus, along with the changes of θ_2 and θ_1, (25) can be regarded as a LPV system with respect to $\cos(\theta_2-\theta_1)$. This article uses the values of $\cos(\theta_2-\theta_1)$ at different angles to design the gain scheduled controller so as to improve the control performance. However, it is difficult to design a gain scheduled controller by using the polytope technique for a LPV system with a structure of (25). A 1st-order filter (6) is thus introduced in this paper to solve the problem. The coefficient matrices take the following form: $A_u=diag\{-h,-h\}$, $B_u=diag\{d_1,d_2\}$ and $C_u=diag\{l,l\}$.

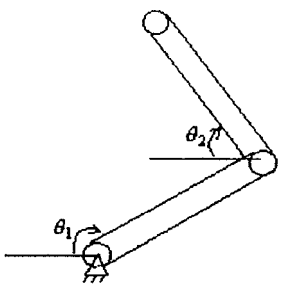

Fig. 5. The structure schematic drawing of the direct-drive robotic manipulator.

h,d_1,d_2 and l are the filter design parameters. Define $x=[\hat{x}\ \ x_u]^T$. By combining (6) and (25), the augmented system can be expressed as

$$\dot{x}=\tilde{A}x+\tilde{B}u \quad (26)$$

where $\tilde{A}=\begin{bmatrix}0&0&1&0&0&0\\0&0&0&1&0&0\\0&0&0&0&\dfrac{l}{a}&-\dfrac{bl}{ac}\cos(\theta_{2e}-\theta_{1e})\\0&0&0&0&-\dfrac{bl}{ac}\cos(\theta_{2e}-\theta_{1e})&\dfrac{l}{c}\\0&0&0&0&-h&0\\0&0&0&0&0&-h\end{bmatrix}$

and $\tilde{B}=\begin{bmatrix}0&0\\0&0\\0&0\\0&0\\d_1&0\\0&d_2\end{bmatrix}$.

It is seen that after the introduction of the filter, $\tilde{A}$ becomes a linear function of $\cos(\theta_{2e}-\theta_{1e})$. For such a structure, the polytopic technique can be used to design the gain scheduled controller. Let $\rho=-\dfrac{bl}{ac}\cos(\theta_{2e}-\theta_{1e})$. Such a selection of ρ makes the system have only one varying-parameter so that the design is simplified. From Figure 5, $\theta_{2e}-\theta_{1e}\in[-\pi,0]$. Thus, $\rho\in[\rho_{\min},\rho_{\max}]=\left[-\dfrac{bl}{ac},\dfrac{bl}{ac}\right]$. Since $\dfrac{\rho_{\max}-\rho}{\rho_{\max}-\rho_{\min}}+\dfrac{\rho-\rho_{\min}}{\rho_{\max}-\rho_{\min}}=1$, let $\mu_1(\rho)=\dfrac{\rho_{\max}-\rho}{\rho_{\max}-\rho_{\min}}$ and $\mu_2(\rho)=\dfrac{\rho-\rho_{\min}}{\rho_{\max}-\rho_{\min}}$. Such a selection of μ_1 and μ_2 makes the system have a convex property. After a convex decomposition, the augmented system (26) can be expressed in a polytopic form as

$$\dot{x}=\left\{\sum_{i=1}^{2}\mu_i(\rho)A_i\right\}x+\tilde{B}u \quad (27)$$

where $A_1=\begin{bmatrix}0&0&1&0&0&0\\0&0&0&1&0&0\\0&0&0&0&\dfrac{1}{a}&\rho_{\min})\\0&0&0&0&\rho_{\min}&\dfrac{1}{c}\\0&0&0&0&-h&0\\0&0&0&0&0&-h\end{bmatrix}$

https://doi.org/10.1017/S0263574703005071 Published online by Cambridge University Press

and $A_2=\begin{bmatrix} 0 & 0 & 1 & 0 & 0 & 0 \\ 0 & 0 & 0 & 1 & 0 & 0 \\ 0 & 0 & 0 & 0 & \frac{1}{a} & \rho_{\max} \\ 0 & 0 & 0 & 0 & \rho_{\max} & \frac{1}{c} \\ 0 & 0 & 0 & 0 & -h & 0 \\ 0 & 0 & 0 & 0 & 0 & -h \end{bmatrix}$.

It is seen clearly that $\mu_1(\rho)$ and $\mu_2(\rho)$ are polytopic coordinates, i.e., $\mu_1(\rho)>0$, $\mu_2(\rho)>0$ and $\mu_1(\rho)+\mu_2(\rho)=1$.

With the consideration of the disturbance $w(t)$ and the performance index $Z(t)$, a polytopic LPV system as (8) can be obtained by combining (27), where

$$A(\rho)=\sum_{i=1}^{2}\mu_i(\rho)A_i\ B_2=\tilde{B},\ B_1=\begin{bmatrix} 0 & 0 \\ 0 & 0 \\ 1 & 0 \\ 0 & 1 \\ 0 & 0 \\ 0 & 0 \end{bmatrix},$$

$$C_1=\begin{bmatrix} \sqrt{q_1} & 0 & 0 & 0 & 0 & 0 \\ 0 & \sqrt{q_2} & 0 & 0 & 0 & 0 \\ 0 & 0 & \sqrt{q_3} & 0 & 0 & 0 \\ 0 & 0 & 0 & \sqrt{q_4} & 0 & 0 \\ 0 & 0 & 0 & 0 & 0 & 0 \\ 0 & 0 & 0 & 0 & 0 & 0 \end{bmatrix},$$

$$D_{12}=\begin{bmatrix} 0 & 0 \\ 0 & 0 \\ 0 & 0 \\ 0 & 0 \\ \sqrt{q_5} & 0 \\ 0 & \sqrt{q_6} \end{bmatrix}$$

and $q_i\geq 0$ $(i=1, 2, 3, 4, 5, 6)$ are weighting factors.

Thus, for the planar two-joint direct-drive robotic manipulator, we can design, according to Section 3, a polytopic gain scheduled state feedback controller (10), which guarantees the quadratic D-stability of the closed-loop system and the quadratic H_∞ performance γ between the external disturbance $w(t)$ and the performance index $Z(t)$ for the whole range of the varyingparameter ρ. Here $N=2$, i.e., $K(\rho)=\sum_{i=1}^{2}\mu_i(\rho)K_i$ and K_i is the vertex of the polytopic controller.

In our experiments, according to the real situation of the robotic manipulator, the parameters of the filter are chosen as $h=20$, $d_1=1$, $d_2=1$ and $l=20$. The weighting factors in the performance index $Z(t)$ are chosen as $q_1=2.25$, $q_2=9$, $q_3=1$, $q_4=16$, $q_5=1.44$ and $q_6=1{,}44$. The system's closed-loop poles are required to be placed in the region of $\alpha=1$, $r=20$ and $\theta=\pi/4$. By using the command "mincx" in MATLAB *LMI Control Toolbox* to optimize the LMIs in Theorem 3, an optimized $\gamma=1.0248$ can be obtained. The state feedback gain matrices for the polytopic vertices are designed, respectively:

$$K_1=\begin{bmatrix} 123.6096 & -10.8670 & 78.2676 & -0.9341 & 9.1816 & -9.0301 \\ -3.5177 & 70.7212 & -0.0010 & 29.5344 & -3.6809 & 11.5475 \end{bmatrix}$$

$$K_2=\begin{bmatrix} 123.6096 & 10.8670 & 78.2676 & 0.9341 & 9.1816 & 9.0301 \\ 3.5177 & 70.7212 & 0.0010 & 29.5344 & 3.6809 & 11.5475 \end{bmatrix}$$

The closed-loop poles corresponding to the vertices are:

$$\{-16.7693\pm 8.6555i, -15.2977, -5.4949, -4.3245, -2.0736\}.$$

It is seen that the designed controller not only satisfies the pole-placement requirements, but also has a good H_∞ performance due to a small optimized γ. After the design of the vertices' controllers for the polytope, the overall polytopic controller satisfying Theorem 2 can be obtained from (10). Figure 6 demonstrates the design principle of the controller.

In our experiment, a square wave and a sinusoid wave are used as reference inputs. The square wave is used to test the switching ability as well as the stability and dynamic characteristics of the system. The reference inputs for joint 1 and joint 2 are a square wave with a frequency of 0.125 Hz and a sinusoidal wave, i.e., $\theta_{2d}=0.5+0.5\sin(0.25\pi t)$, respectively. By using the proposed polytopic controller (10), the joint position response and the control torque curves are shown in Figure 7. A comparison between the proposed controller and the single H_∞ LTI controller is made and the resulted responses are also shown in Figure 7.

It is seen from Figure 7(a) that under the functioning of the polytopic gain scheduled H_∞ controller, the robotic manipulator has no overshooting, a smooth motion and a small rise time in its step response. Also, the system has a

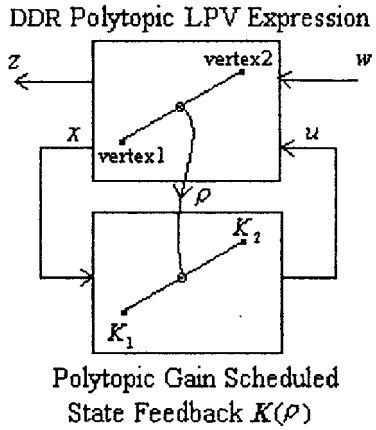

Fig. 6. The design principle of the polytopic controller for the direct-drive manipulator.

https://doi.org/10.1017/S0263574703005071 Published online by Cambridge University Press

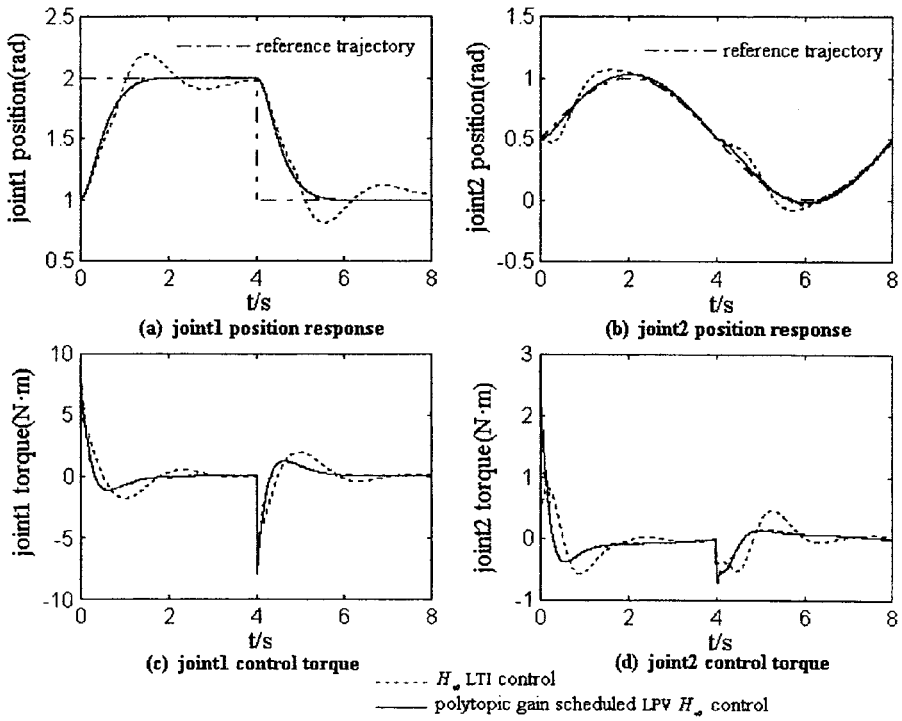

Fig. 7. Experimental results.

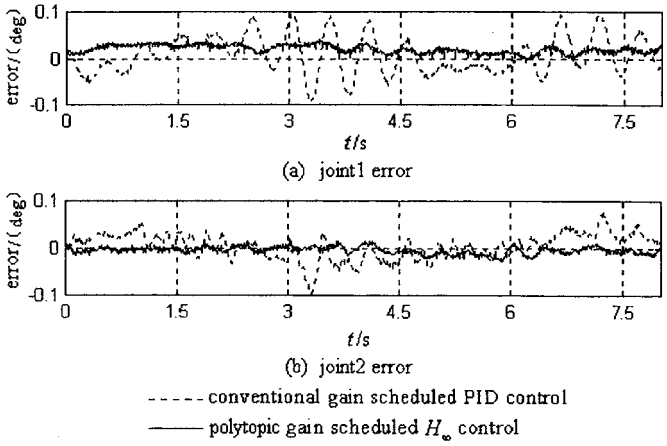

Fig. 8. Experimental results for tracking.

strong switching ability between different points. It is evident that the step response under the functioning of a single H_∞ LTI controller is much worse. Figure 7(b) demonstrates that though there is a distortion in the response at the 4th second due to a sudden increase of the load on joint 2 as a result of the position switching of joint 1, the manipulator catches up the reference input right away under the functioning of the polytopic gain scheduled H_∞ controller. The spikes in Figure 7(c) are corresponding to the boundaries of the square wave input, while those for joint 2 shown in Figure 7(d) are due to the large impulse on joint 2 as a result of the sudden position switching of joint 1.

Also, we did a tracking experiment. Let the end-effector of the manipulator track a circle of radius 0.6 m with a speed of 1 m/s. The coordinates of the center of the circle is (0.40 m, 0.30 m). The joint errors are recorded. Figure 8 demonstrates a comparison of the control performance between the proposed controller and the conventional gain scheduled PID controller. It is seen that the maximum errors for joints 1 and 2 under the conventional gain scheduled PID controller are 0.1°, respectively, with evident vibration, while those under the proposed gain scheduled controller are 0.04° and 0.03°, respectively, without any vibration. Thus, a better control performance is demonstrated.

5. CONCLUSIONS

Thanks to the introduction of the polytope technique, the design of a controller is transformed into a design of the vertices' controllers for the polytope in this paper. The deficiency of the conventional gain scheduled controller, i.e., a big computation load, working only for a slow varying system, and a lack of theoretical guarantee of system stability and performance in the whole range of the varying-parameter, is overcome. With a combination of a H_∞ design and pole placement, the designed controller has the performance of disturbance attenuation, robust stability and fast dynamics resistance. It is feasible to digital realization. In order to transform the linearized robotic state equation to be a polytopic expression, which is liable to the design of a gain scheduled controller, a 1st-order filter is introduced. The design of the vertices' controllers is the key to the polytopic gain scheduled H_∞ controller design. The LMI technique is used in this paper to obtain the desired optimized solution. The proposed polytopic gain scheduled H_∞ controller is applied to a two-joint direct-drive robotic manipulator. Experiment results demonstrate the tracking ability of the system. System stability is proved by the performance of the system under a fast switching of a square wave. Comparisons with the performance of the H_∞ LTI controller and the conventional gain scheduled PID

https://doi.org/10.1017/S0263574703005071 Published online by Cambridge University Press

controller demonstrate the superiority of the proposed polytopic gain scheduled H_∞ controller.

References

1. J.C. Doyle and G. Stein, "Multivariable feedback design: concepts for a classical/modern synthesis", *IEEE Trans. on Automatic Control* **26**(1), 4–16 (1981).
2. P. Apkarian and R.J. Adams, "Advanced gain-scheduling techniques for uncertain systems", *IEEE Trans. on Control Systems Technology* **6**(1), 21–32 (1998).
3. M.S. Queiroz, D.W. Dawson and M; Agarwal, "Adaptive control of robot manipulators with controller/update law modularity", *Automatica* **35**(7), 1379–1390 (1999).
4. Y. Tang and M.A. Arteaga, "Adaptive control of robot manipulators based on passivity", *IEEE Trans. on Automatic Control* **39**(9), 1871–1875 (1994).
5. B. Chen, "A nonlinear H_∞ control design in robotic systems under parameter perturbation and external disturbance", *Int. J. of Control* **59**(2), 439–461 (1994).
6. Y. Choi, "Robust control of manipulators using Hamiltonian optimization", *Proc. of the IEEE Int. Conf. on Rob. and Autom*., Albuquerque, New Mexico (1997) pp. 2358–2364.
7. K. Watanabe, "A nonlinear robust control using a fuzzy reasoning and its application to a robot manipulator", *J. of Intelligent and Robotics Systems* **20**(2), 275–294 (1997).
8. A. Karakasoglu, "A recurrent neural network-based adaptive variable structure model-following control of robotic manipulator", *Automatica* **31**(10), 1495–1507 (1995).
9. J.S. Shamma and M. Athans, "Analysis of nonlinear gain scheduled control systems", *IEEE Trans. on Automatic Control* **35**(8), 898–907 (1990).
10. J S. Shamma and M. Athans, "Gain scheduling: potential hazards and possible remedies", *IEEE Control Systems* 101–107 (June, 1992).
11. J. Jiang, "Optimal gain scheduling controller for a diesel engine", *IEEE Control System* 42–48 (August 1994).
12. P. Gahinet and P. Apkarian, "A Linear matrix inequality approach to H_∞ control", *J. of Robust and Nonlinear Control* **4**, 421–448 (1994).
13. Y. Nesterov and A. Nemirovski, "An interior-point method for generalized linear-fractional problems", *Math. Programming* **Ser. B** (1996).
14. P. Gahinet, N. Arkadii *et al*. "The LMI control Toolbox", *Proc. of 33rd Conf. on Decision and Control*, Lake Buena Vista, Florida (Dec. 1994) pp. 2038–2041.
15. M. Chilali and P. Gahinet, "H_∞ design with pole placement constraints: an LMI approach", *IEEE Trans. on Automatic Control* **41**(3), 358–367 (1996).
16. Z.-W. Yu and H.-T. Chen, "Friction adaptive compensation scheme based on sliding-mode observer", *Robot* **21**(7), 562–568 (1999).

https://doi.org/10.1017/S0263574703005071 Published online by Cambridge University Press